nature climate change

ARTICLES

PUBLISHED ONLINE: 5 OCTOBER 2015 | DOI: 10.1038/NCLIMATE2811

Physiological responses of a Southern Ocean diatom to complex future ocean conditions

P. W. Boyd[1,2*], P. W. Dillingham[3], C. M. McGraw[3,4], E. A. Armstrong[5], C. E. Cornwall[1,6†], Y.-y. Feng[6†], C. L. Hurd[1,6], M. Gault-Ringold[7†], M. Y. Roleda[6†], E. Timmins-Schiffman[8] and B. L. Nunn[8]

A changing climate is altering many ocean properties that consequently will modify marine productivity. Previous phytoplankton manipulation studies have focused on individual or subsets of these properties. Here, we investigate the cumulative effects of multi-faceted change on a subantarctic diatom *Pseudonitzschia multiseries* by concurrently manipulating five stressors (light/nutrients/CO_2/temperature/iron) that primarily control its physiology, and explore underlying reasons for altered physiological performance. Climate change enhances diatom growth mainly owing to warming and iron enrichment, and both properties decrease cellular nutrient quotas, partially offsetting any effects of decreased nutrient supply by 2100. Physiological diagnostics and comparative proteomics demonstrate the joint importance of individual and interactive effects of temperature and iron, and reveal biased future predictions from experimental outcomes when only a subset of multi-stressors is considered. Our findings for subantarctic waters illustrate how composite regional studies are needed to provide accurate global projections of future shifts in productivity and distinguish underlying species-specific physiological mechanisms.

An ongoing major challenge is to grasp how climate-change-mediated alteration of environmental conditions will influence biota across different scales, from organismal health to community structure[1,2]. Oceanographers have employed climate-change models[3,4], time-series observations[5] and manipulation experiments[6] to understand the biological ramifications of global change. Phytoplankton manipulation studies reveal how alteration of individual properties, such as CO_2, affects physiology[2,6,7]. However, the validity of such single-parameter findings[6,8,9], in the context of complex ocean change[1,2], is challenged by research that reveals interactive effects between multi-stressors on phytoplankton physiology[10,11]. We need to diagnose and understand the physiological mechanisms that underpin interconnected responses to multi-stressors, which together set the cumulative response of phytoplankton species to changing conditions[4,6,8].

Understanding the combined effects, across the global ocean, of complex change on phytoplankton physiology requires a gradualist approach[12,13]. Individual provinces will encounter different permutations of multi-faceted change[14], and each is characterized by a range of resident phytoplankton groups (termed biomes[5]). Earth System models provide a framework of projections of regional change[14] that stimulate improved experimental design to understand the biological effects of oceanic change. In return, a new generation of manipulation studies must deliver estimates of the combined effects of complex change on many phytoplankton species, and distinguish the underlying mechanisms that underpin these physiological outcomes.

Here, we target subantarctic diatoms, which are ubiquitous and bloom-formers[15]. We experimentally manipulate a representative species[6,15] (*Pseudonitzschia multiseries*) under year 2100 conditions to quantify its response to ocean change. For simplicity, owing to the complex nature of our multi-stressor experiment, we chose batch cultures that permit initial (high nutrient) conditions to be modified biologically but require careful monitoring. Our experimental design, along with physiological metrics and comparative proteomics, enables diagnosis of individual and interactive effects of ocean properties on diatom physiology. Thus, regionally we can quantify the cumulative effect of complex change, and begin to identify underlying physiological mechanisms, as a first step towards re-evaluation of climate-change biogeochemical model parameterizations and experimental designs[3,4,13].

Experimental design

We commence by outlining a new experimental design that relies on recognition of the controlling physiological variable for the study organism. Fullest interpretation of results requires the application of many physiological diagnostics, together with a statistical approach that is powerful enough to unravel the relative contribution of individual and interactive environmental effects on our diatom. At present, even sophisticated experiments[10,11] manipulate only subsets of properties projected to change by 2100 (refs 1–4).

[1]Institute for Marine and Antarctic Studies, University of Tasmania, Hobart, 7005 Tasmania, Australia. [2]Antarctic Climate and Ecosystems Cooperative Research Centre, University of Tasmania, Private Bag 80, Hobart, Tasmania 7001, Australia. [3]School of Science and Technology, University of New England, Armidale, 2351 New South Wales, Australia. [4]Gustaf H. Carlson School of Chemistry, Clark University, Worcester, Massachusetts 01610, USA. [5]NIWA/University of Otago Research Centre for Oceanography, Department of Chemistry, University of Otago, Dunedin 9054, New Zealand. [6]Department of Botany, University of Otago, PO Box 56, Dunedin 9054, New Zealand. [7]Department of Chemistry, University of Otago, PO Box 56, Dunedin 9054, New Zealand. [8]Department of Genome Sciences, Box 355065, University of Washington, Seattle, Washington 98195, USA.
†Present addresses: School of Earth and Environment & ARC Centre of Excellence for Coral Reef Studies, The University of Western Australia, Crawley, 6009 Western Australia, Australia (C.E.C.); Tianjin University of Science and Technology, Tianjin 300457, China (Y.-y.F.); Antarctic Climate and Ecosystems Cooperative Research Centre, University of Tasmania, Private Bag 80, Hobart, Tasmania 7001, Australia (M.G.-R.); Norwegian Institute for Bioeconomy Research, Kudalsveien 6, 8049 Bodø, Norway (M.Y.R.). *e-mail: philip.boyd@utas.edu.au

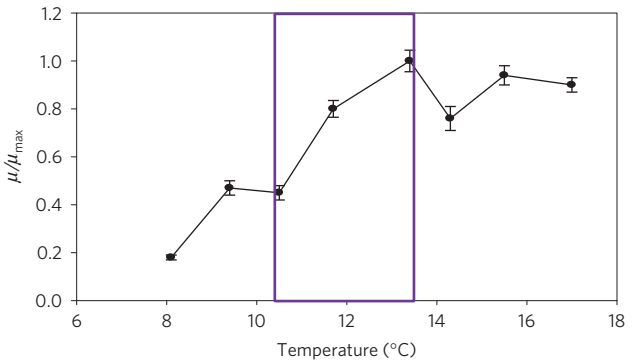

Figure 1 | A reaction norm of *P. multiseries*, expressed as growth rate at each temperature divided by maximum observed growth rate for the norm. The norm substantiated temperature as the dominant physiological control on subantarctic diatoms following our arbitrary selection criteria. Error bars denote ±s.d. of the mean ($n=3$), and the temperature bounds of the purple rectangle denote the mean (10.6 °C) for subantarctic surface waters for present-day spring/summer[29,46] used in treatments A and C, and that projected (13.7 °C) for this province by 2100 (ref. 18) and used in B and D. Doubling of growth from 10.6 to 13.7 °C reveals that selection of these temperatures cause the largest increase in growth rate per °C warming, relative to present-day temperature. Thus, the role of warming in setting growth of this subantarctic diatom will be time-dependent and may decrease beyond 2100 unless diatoms can respond by altering their thermal traits[47].

To address the dual issues of quantification of the cumulative effects of complex change and its mechanistic underpinning, we require an experiment that supersedes present-day single- or 2–3-parameter manipulations. We employed a collapsed factorial design that provides a tractable, efficient, approach while concurrently manipulating the stressors that exert major physiological controls (temperature/CO_2/nutrients/iron/light[6]). This streamlined design requires identification of the dominant physiological control[16] before grouping (that is, collapsing) the remaining stressors into one combined factor (Methods).

In the Southern Ocean, temperature is recognized as setting the upper bound on diatom growth[17]. For *P. multiseries*, we used a literature-based physiological ranking[6] to identify temperature as the (putative) dominant control. Its pivotal role for our subantarctic diatom was substantiated by a reaction norm that revealed twofold higher growth (Fig. 1), on 3 °C warming projected for 2100 (refs 3,4,18); note, this corroboration is contingent on our selection criteria (Fig. 1 caption) and different outcomes are possible if other metrics are applied. The remaining parameters (CO_2/nutrients/iron/light) were then grouped into a combined factor. Next, we employed a 2^2 factorial design with four treatments (Fig. 2): (A) control; (B) 2100 warming only[18]; (C) 2100 conditions without warming; (D) 2100 conditions[18] (Table 1). Our approach balances the needs of predicting cumulative physiological effects of future conditions with identifying the nature of environmental forcing. This method led to improved efficiency in experimental design (2^2 compared with 2^5 treatments for 5-factors), and the orthogonality of the dominant physiological control with the collapsed stressors permits identification of how much variation is explained by temperature alone, the collapsed stressors, and their interplay.

Growth rate and cell counts, which integrate organismal health, were defined as primary physiological metrics. Secondary diagnostics and comparative proteomics[19,20] provide further mechanistic insights into how organismal performance is environmentally forced. Interpretation of the relative roles of individual versus interactive effects of stressors on our diatom were explored by cross-comparing experimental outcomes in conjunction with Akaike's information criterion (AIC) and partial-R^2 (Methods). AIC enables identification of the relative importance of individual factors, and their interplay, by assessing how well different statistical models fit the physiological data sets[21]. Inter-comparison of the physiological effects of each treatment enables the following diagnoses: individual effect of future warming (B versus A); cumulative effects of future change (D versus A); interactive effects of a future ocean (without warming; C versus A); complex interplay of warming with altered properties ((D versus B) compared with (C versus A)) (Fig. 2).

To inter-compare physiological effects, model averaging is the recommended statistical approach[21]. Specifically, we considered five statistical linear regression models for model averaging using AIC: (M1) a null model with no treatment effects; that is, all treatments have a common response for the metric (for example, identical growth rates); (M2) a model with only temperature effects; (M3) a model with only collapsed multi-stressors effects; (M4) a model with effects for temperature and the collapsed multi-stressors, but no interactions (that is, the response is determined by summing the effects of temperature and the collapsed multi-stressors); (M5) a model with different responses for each treatment, comprising effects of temperature, the collapsed multi-stressors, and their interactions.

Experimental results

Figure 3 reveals wide-ranging physiological responses across treatments A–D. As anticipated (Fig. 1), the individual effect of warming (B) significantly increased (chlorophyll-based) growth from 0.49 ± 0.05 to $0.75 \pm 0.05\ d^{-1}$. However, the effect of warming alone on other metrics was either small (cellular chlorophyll, Si) or inconclusive. In C, despite higher iron, p_{CO_2} and irradiance, contrasting trends were evident: growth was $0.37 \pm 0.05\ d^{-1}$, cellular chlorophyll increased sixfold, and cellular N and P increased fivefold. In D, where warming was one of five altered multi-stressors, more pronounced patterns emerged. Growth ($0.99 \pm 0.09\ d^{-1}$) doubled and substantial decreases were observed for cellular P and Si (compared with treatment A, Fig. 3). Model-averaged estimates of inter-comparisons of physiological effects show striking differences for individual and interactive effects of warming and other multi-stressors across these metrics (Supplementary Table 2).

The trends observed in treatment D are explained by the complex interplay between warming and the other stressors ((DB) compared with (CA)): positive for growth and cell counts, but negative for other physiological responses (cellular chlorophyll, N, P; Supplementary Table 2). The importance of considering all five stressors when assessing their effect on cellular elemental composition is also apparent from the ratios of metrics (Supplementary Table 3). Although differences in C/chlorophyll and Si/N ratios were observed across A–C, similar values were observed in these treatments for C/N, C/P and N/P. When all stressors were manipulated (treatment D), N/P increased, C/N decreased and C/chlorophyll was the lowest recorded, emphasizing the value of monitoring multiple physiological responses.

The influential role of temperature on our primary diagnostics is confirmed in Fig. 4, where temperature explains 80% of the variation in growth and 53% for cell counts. However, Fig. 4 also reveals that temperature alone is insufficient for accurately predicting the diatom response to complex change. When light/iron/nutrients/CO_2 and their interplay with temperature are included, >90% of the variation in the metrics is explained (Fig. 4 and Supplementary Table 4). This conclusion that temperature is the dominant control for this diatom species, and that interactive effects are important, is reinforced by AIC weights, which reveal >99% support for statistical model M5 (Supplementary Table 4). Figure 4 shows that the effects of light/iron/nutrients/CO_2, either

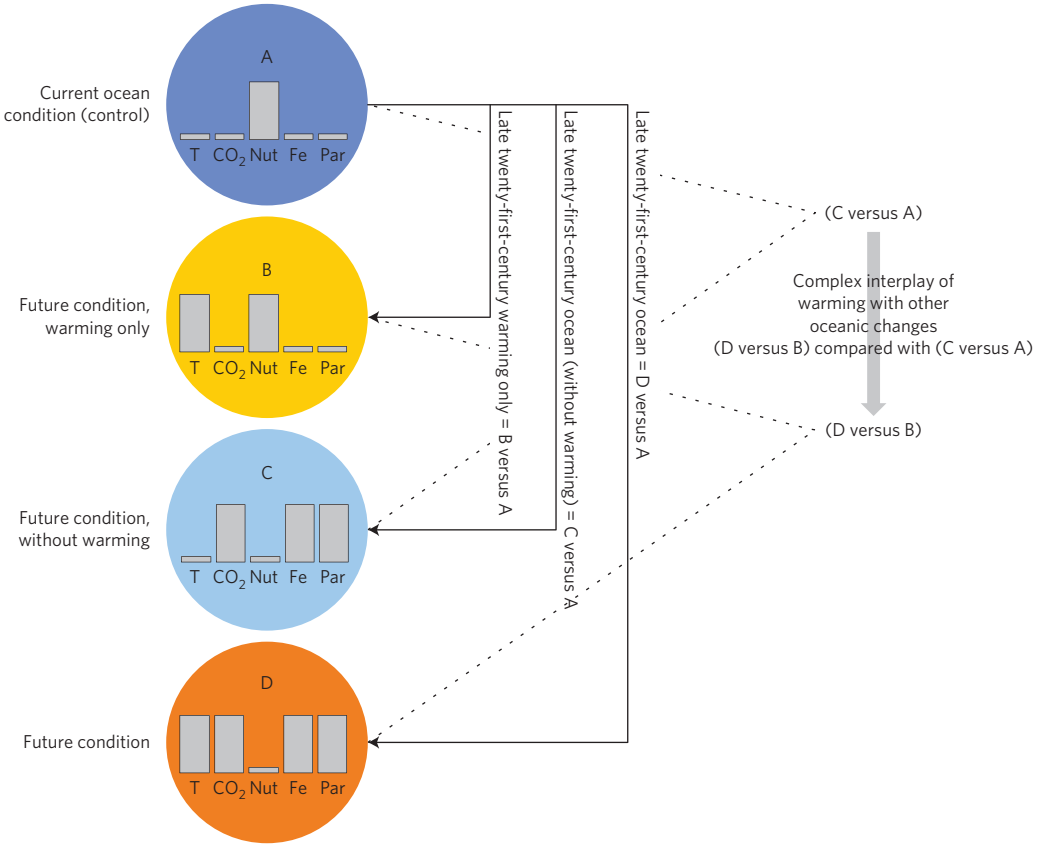

Figure 2 | Experimental design to mimic a future ocean and assess the individual and interactive physiological effects of temperature. Each bar graph (bars not to scale) graphically illustrates relative changes in each of five biologically influential properties across four treatments as detailed in Table 1. The arrows (and accompanying text) that link the treatments describe how the individual and interactive effects of warming on diatom physiology are teased apart. Future changes to each property for subantarctic waters were obtained from regional model projections from a global climate-change model[18,46] (see Methods).

Table 1 | Summary of the experimental media (nutrients and iron) and conditions (light, temperature, CO_2) employed for treatments A–D, in relation to model projections[18,46] for subantarctic waters for year 2100.

Property	Medium 1 (treatments A and B)	Medium 2 (treatments C and D)	Subantarctic model projections[18,46]
Nutrients (μM)	300 NO_3:20 PO_4:100 Si	210 NO_3:14 PO_4:70 Si	Future supply 30% less than present day
Iron*†	20 (pFe) [Fe′] = 51.7 (A) and 62.8 (B) pmol l^{-1}	19.1 (pFe) [Fe′] = 244.5 (C) and 205.2 (D) pmol l^{-1}	Iron ~2-fold higher than present day
CO_2 (expressed as DIC, μmol kg^{-1})	2,245 (±31)	2,372 (±7)	Future CO_2 ~double present day
Temperature	10.6±1°C (treatment A) 13.7±1°C (B)	10.6±1°C (treatment C) 13.7±1°C (D)	Future ~3 °C warmer than present day
PAR (μmol quanta m^{-2} s^{-1})	30±6 (continuous)	55±7 (continuous)	Future higher than present day for mean mixed-layer irradiances for subantarctic waters south of New Zealand

The magnitudes of the nutrient additions and CO_2 enrichment were confirmed by analysis (Supplementary Table 1, Methods). *Denotes calculations of free iron concentration (Fe′), to take into account the combined effects of pH, irradiance and temperature[39] in treatments A–D (see Supplementary Methods). †Denotes that the iron enrichment was higher than the model projections[18] but that it represented iron-replete (>200 pM) relative to iron-deplete (<200 pM) conditions for subantarctic waters[29]. Alteration of ocean properties (by year 2100) were based on regional projections from the NCAR Community Earth System Model biogeochemical climate-change model[18,46].

individually or together explain little of the variability in the primary diagnostics. As iron enrichment can significantly enhance subpolar diatom growth[6,10,15], its beneficial influence may be offset by negative effects due to fewer nutrients. Similar trends, with respect to warming, were also observed for most secondary diagnostics (Fig. 4), whereas cellular chlorophyll and Si may respond more to changes in other stressors (individually and/or interactively) when combined with warming.

Visualization of proteomic (Data set 1) and physiological measurements (Supplementary Table 2) across treatments A–D was based on two multivariate analyses (non-metric multidimensional scaling: NMDS; and principal component analysis: PCA; Fig. 5). Both analyses project high-dimensional data (that is, abundances of 1,640 proteins or multiple physiological responses) onto a new set of axes (ordinations), where the x axis explains the greatest variation in the original data and the y axis explains the second greatest variation. Coordinates/ordinations of A–D in Fig. 5 illustrate that the proteomic responses can be correlated with the physiological metrics along both axes, linking molecular-level measurements with phenotypic observations. Examination of metabolic processes of

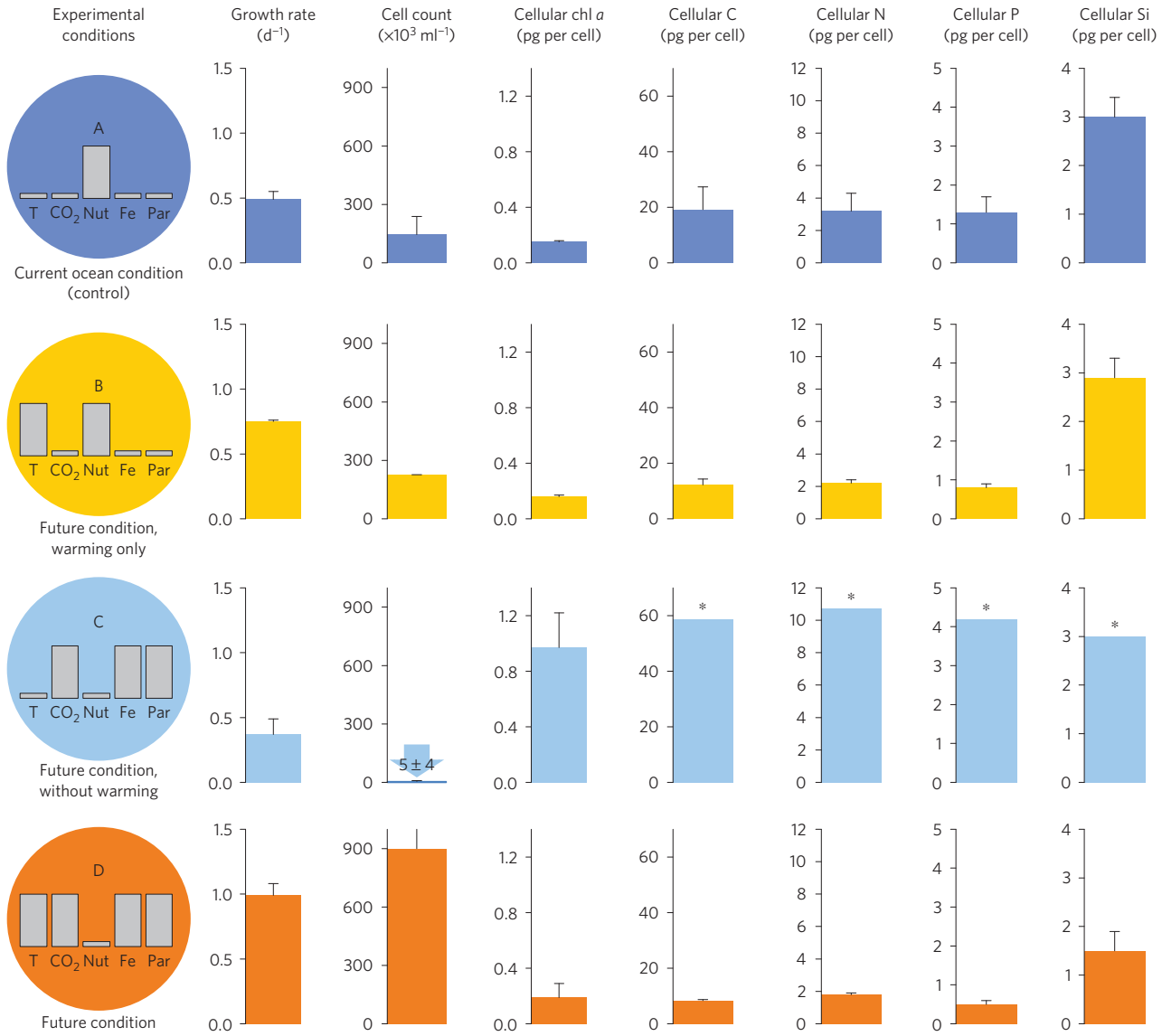

Figure 3 | Summary of physiological metrics sampled during exponential growth (Supplementary Fig. 1) from each of treatments A–D (represented again by bar graphs within colour-coded circles depicting culture conditions detailed in Table 1). Error bars are the s.d. of the mean ($n=3$). *Denotes data from one C treatment where some assays were at the limit of detection (that is, lower than the blank) owing to the weak physiological response. No significant change in cell size was observed across treatments A–D. Note, batch cultures for treatments A–D were each sampled/collected during exponential growth (Supplementary Fig. 1) and hence cells were not resource-limited. At the experiment's conclusion, pronounced decreases in phosphate and increases in pH were evident in D, suggesting resource limitation (Supplementary Table 1). However, the physiological ramifications of these shifts are probably minor on the basis of reported plasticity of laboratory-cultured *P. multiseries* in response to increased pH (to 8.4; ref. 48), and bloom-forming diatoms that were not P-limited in batch cultures at ~0.5 μmol PO_4 l^{-1} (ref. 49).

proteins that describe the greatest observed variance (NMDS1 axis, Fig. 5a) revealed that relative abundances of proteins responsible for transcription and translation separated treatment C from the others, whereas PCA along the PC1 axis shows separation of A–D based on cell counts, cellular content, and growth. PC2 exhibits additional separation by chlorophyll and cellular Si. Together, both plots suggest that the isolation of treatment C is partially due to our diatom's inability to process and translate RNA.

More specifically, the significant difference in cellular P across treatments A–D (Fig. 3) correlates with the abundance of proteins involved in translational processes that utilize P-rich macromolecules (RNA to protein; fewer in D compared with A; more in C compared with A, Fig. 5a). Figure 5a also reveals temperature-driven proteome alterations, such as a metabolic strategy supporting increased growth in B (compared with A) that is evident from 1.5-fold higher abundances of a global transcriptional regulator/cell division control protein (Data set 1). Under late twenty-first-century conditions (treatment D), other strategies are conspicuous (for example, photosynthetic complex proteins are significantly more abundant relative to the control; Fig. 5a). There is also evidence of temperature-driven intracellular reactions dictating proteome responses between both future conditions, with (D) and without warming (C).

Discussion

Individual versus interactive effects. The individual effect of warming on subantarctic *P. multiseries* physiology was compared with published studies (Supplementary Table 5). Warming influences subpolar diatoms in different ways, including increasing cellular chlorophyll[22,23], carbon[22,23], C/N ratios[22] and growth[23], but

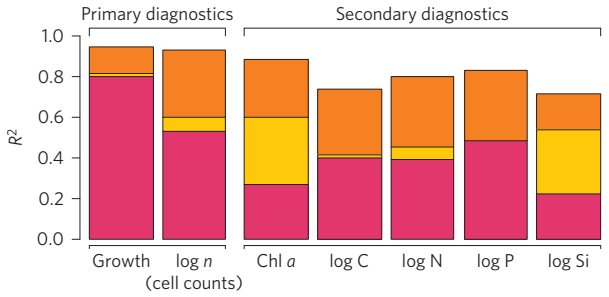

Figure 4 | Individual versus the interactive physiological effects of warming on our study diatom. The proportion of variation (R^2) explained by temperature (pink, lower), the other altered properties (p_{CO_2}/PAR/Fe/nutrients) (light orange, middle) and their interaction (dark orange, top) for: the primary metrics of growth (d^{-1}) and cell abundance (n); and the secondary metrics of cellular chlorophyll, C, N, P and Si.

decreasing both cellular P (ref. 24) and cell size[25,26]. Here, warming resulted in increased growth rate and cellular chlorophyll (Fig. 3). The differentially abundant proteins in treatments A versus B were enriched for B in processes involved mostly in intracellular transport (for example, vesicle coat complex AP-2, clathrin adaptor complex, and inner membrane protein translocase, Data set 1). This is indicative of greater intracellular protein transport and turnover when diatoms are exposed to warming[27].

The metric for maximum growth (μ_{max}) as a function of temperature[28] provides insights into the relative roles of warming and other stressors for our diatom species. Although temperature sets the upper bound on Southern Ocean phytoplankton growth[17], iron-enrichment[6,29] and/or nutrient stress or limitation[30] can modify rates and influence μ/μ_{max}. As expected, our low-iron control showed submaximal growth (0.5 d^{-1} compared with 1.1 d^{-1} predicted μ_{max} (ref. 28) at 10.6 °C). Future warming in B increased growth to submaximal rates (0.75 d^{-1} compared with 1.3 d^{-1} μ_{max} at 13.7 °C) revealing that other factors either individually/or interactively restricted growth. The influence of these stressors on growth is evident from statistical modelling (Fig. 4), and from D, which had the highest rate (0.99 ± 0.05 d^{-1}). Despite using batch cultures, submaximal growth in D is more likely to be influenced by the individual/interactive effects of 30% less macronutrients for future subantarctic waters[18] than higher CO_2/irradiances that each have either negligible[25] or positive[23] effects on diatom growth, respectively.

Our collapsed factorial design enables quantification of individual and interactive effects of temperature, but requires inferences to be made into the interplay of temperature and other stressors. Diagnosis of this interplay relied on a comparison of physiological trends from treatments C and D with studies where individual[26] and/or several[25] properties (temperature/p_{CO_2}, iron/p_{CO_2} were manipulated (Supplementary Table 5). For example, iron enrichment increases diatom growth[26,31] as does higher light (under iron-replete conditions[23]), whereas higher p_{CO_2} does not[25], providing evidence of their relative contribution (above that of warming) to increased growth in treatment D relative to B. Iron enrichment[31] or warming[24] each decrease diatom cellular P (increasing N/P ratios), whereas CO_2 does not alter N/P (Supplementary Table 5), offering robust interpretations of observed changes in this metric in treatment D compared with A. Decreased cellular P in treatment D is consistent with fewer translational process (RNA to protein) proteins per cell in treatment D (compared with A) compared with C (compared with A) (Fig. 5a, Data set 1). For cellular Si, diatoms in treatment D had ~50% of the Si content of cells in A–C. This trend is not solely temperature-driven (Fig. 4), and probably also due to decreased Si requirements under lower silicate concentrations[32]

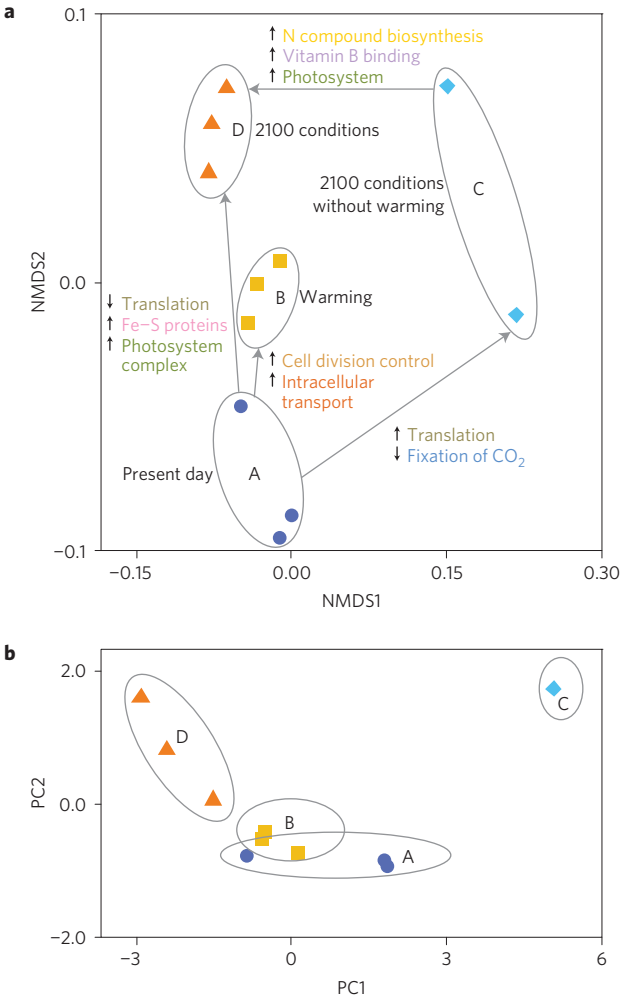

Figure 5 | Representations of the different outcomes of treatments A–D. **a**, Proteomics. **b**, Physiological metrics. Biological replicates in treatment A are denoted by blue circles; B: yellow squares; C: light blue diamonds ($n=2$ in **a**, and $n=1$ in **b** owing to low biomass, see Fig. 3 caption); D: orange triangles. **a**, NMDS analysis of relative protein abundances of 1,640 proteins in treatments A–D. Grey arrows indicate comparisons between treatments: the treatment at the base of the arrow is considered as the 'control' relative to the treatment at the head of arrow. Metabolic processes enriched in the between-treatment protein comparisons are colour-coded to correspond to Data set S1. ↑: metabolic processes with proteins at higher abundance in treatment (versus control); ↓: proteins at lower abundance. Note, little is known about the influence of growth phase on phytoplankton proteomics, with a sole study reporting changes in a small, distinct group of unidentified proteins across different growth phases for a dinoflagellate[50]. **b**, PCA of treatments A–D based on growth rate, cell counts, cellular chlorophyll, C, N, P and Si. PC1 represents 80% of the variation for placement in the data set and PC2 15% of the variation.

and/or iron-mediated decreases in cellular energy metabolism and associated Si uptake[6].

The interplay between stressors ranges from non-interactive cumulative effects to synergistic interplay[8]. Synergistic amplification of growth by warming and iron enrichment (nutrient-replete conditions) is reported for polar diatoms[33], and iron- and CO_2 enrichment (nutrient-replete conditions) synergistically increase N/P ratios, but decrease Si/N ratios of subarctic pennate diatoms[25]. We found direct evidence of positive interactions in our study: 15% and 30% of variations in growth and cell counts, respectively, are explained by the interplay of warming

with other factors (Fig. 4). This prompted investigation of the mechanisms driving these interactions by an inter-comparison of treatments C and D. Low growth in C was initially counterintuitive as C had higher iron, p_{CO_2} and light (but 30% less nutrients).

We propose that the very different outcomes in C and D stem primarily from three inter-related facets primarily involving temperature, iron and nutrients. First, the individual effect of warming on growth (Figs 1 and 4); second, previous reports of individual effects of warming[24,34] and iron enrichment[26,31] on growth; and third the joint influence of temperature (less need for P-rich ribosomal RNA; refs 24,30) and iron (mechanism(s) unknown)[31] in reducing cellular P and partially offsetting any detrimental effects of 30% fewer nutrients in treatment D, or the effects of diatom growth in D ($0.99 \pm 0.09\ d^{-1}$) on nutrient uptake (Supplementary Table 1). Our hypothesis is supported as follows: first eightfold lower cellular P in treatment D compared with C (Fig. 3); second, increased yet submaximal growth (0.99 ± 0.09 compared with $1.35\ d^{-1}$) and F_v/F_m (0.45 compared with 0.65 maximum[35], data not shown) in D suggests that temperature- and/or iron-mediated reduction in cellular elemental requirements partially offsets less nutrients (Supplementary Table 1) and/or their interplay with other stresses. Furthermore, pronounced differences in the outcomes of treatments C and D indicate that the selection of properties to be experimentally manipulated requires great care, as the findings from C (ostensibly a four-way manipulation) yielded unpredicted and misleading conclusions (compared with D for 2100) on diatom responses to complex ocean change. Our evidence for the role of temperature and iron in altering subantarctic diatom physiology, in the context of complex change, was interpreted using physiological and molecular-level syntheses[34,36].

Physiological mechanisms for interactive effects. We propose specific mechanisms for the joint role of warming and iron for enhanced physiological performance in D. Each plays a fundamentally different biochemical role, with temperature reported to accelerate and primarily drive non-enzymatically catalysed reactions[34], whereas iron enhances enzymatically catalysed pathways, including photosynthesis[36]. The summary of metabolic strategies that differentiates treatments A–D in Fig. 5 supports the important interplay between temperature and iron. Together, warming and iron availability boost many biochemical reactions, including photosynthetic ability and electron transfer capacity (supported by >2-fold increased abundance of Rieske [2Fe–2S] protein in D compared with A, Data set 1). The interplay between temperature and iron is further confirmed by proteomic comparison of C and D (Fig. 5a), with more proteins in D (iron enrichment/warming) (compared with C, iron enrichment/no warming) involved in vitamin B binding[37], N compound biosynthesis, and photosystem complexes, all of which require iron (Data set 1).

Figure 5a indicates that the greater photosynthetic capacity of our diatom in D (compared with C) is further evidence of temperature/iron interactions; many of the proteins that increase in abundance in treatment D (compared with C) are involved in photosynthesis and amino acid biosynthesis (Data set 1). Moreover, there is evidence of potential trade-offs between biochemical pathways (translation versus carbon fixation) in treatment C (compared with A), potentially driven by the metabolic shifts necessary to survive in the suboptimal conditions evident in C. Diatoms in C are enriched in ribosomal proteins involved in translation, whereas proteins related to photosynthetic carbon fixation were less abundant (compared with A). These results emphasize the complexity and multi-faceted nature of this diatom species's physiological response to changing conditions.

The disproportionate influence of warming and iron enrichment (and their interplay) on our diatom's physiological response to complex change illustrates the utility of our approach; holistic treatment of multi-stressors to examine their cumulative effect on phytoplankton, followed by exploration of potential causes, to advance subsets of the most influential properties for further scrutiny. In hindsight, our batch culture approach should be superseded by semi-continuous culturing to ensure maintenance of quasi-steady-state conditions in future holistic multi-stressor experiments. In our study, there are likely to be additional interactions between pH and iron[38]; pH and temperature (Supplementary Table 5), p_{CO_2}/iron[10], iron/temperature/light[39] and/or nutrients[6], which may exert subtle effects (for example, altered iron bioavailability[39]). Our approach can stimulate future research, across different ocean biomes, from a holistic standpoint (inclusion of influential multi-stressors) compared with less inclusive (subset of stressors) approaches[6].

Our study reveals that a representative subantarctic diatom species may benefit physiologically by 2100, and that potential doubling of growth rates will alter regional productivity and biogeochemistry[3,4]. This positive response, driven primarily by warming and iron enrichment, may remove the need for adaptive evolution[7] for subantarctic diatoms. Our regional analysis cannot be applied to resident phytoplankton in other provinces, which, depending on their sensitivity to complex change, may respond differently to regionally altered conditions[14]. Nevertheless, our findings demonstrate that diatom physiological responses are driven by both individual and interactive stressors, and not all stressors are equally influential. At present there is incomplete parameterization of many aspects of the physiological interplay, evident here, in climate-change models[3,4,18,40]. However, our study of diatom proteomics interpreted in conjunction with physiological diagnostics points to a compelling biochemical basis that underlies the interplay between stressors. These mechanistic insights set new goals to guide multi-faceted modelling approaches[41] in representing phytoplankton physiology[40] in climate-change models[3,4,18].

Methods

Methods and any associated references are available in the online version of the paper.

Received 24 April 2015; accepted 27 August 2015; published online 5 October 2015

References

1. Doney, S. C. The growing human footprint on coastal and open-ocean biogeochemistry. *Science* **328,** 1512–1516 (2010).
2. IPCC *Climate Change 2014: The Physical Science Basis* (eds Field, C. B. *et al.*) (Cambridge Univ. Press, 2014).
3. Bopp, L. *et al.* Multiple stressors of ocean ecosystems in the 21st century: Projections with CMIP5 models. *Biogeosciences* **10,** 6225–6245 (2013).
4. Dutkiewicz, S., Scott, J. R. & Follows, M. J. Winners and losers: Ecological and biogeochemical changes in a warming ocean. *Glob. Biogeochem. Cycles* **27,** 463–477 (2013).
5. Karl, D. M. *et al.* in *Nitrogen in the Marine Environment* (eds Capone, D. G., Bronk, D. A., Mulholland, M. R. & Carpenter, E. J.) 705–769 (Academic Press, 2008).
6. Boyd, P. W., Strzepek, R. S., Fu, F. X. & Hutchins, D. A. Environmental control of open-ocean phytoplankton groups: Now and in the future. *Limnol. Oceanogr.* **55,** 1353–1376 (2010).
7. Collins, S., Rost, B. & Rynearson, T. A. Evolutionary potential of marine phytoplankton under ocean acidification. *Evol. Appl.* **7,** 140–155 (2014).
8. Boyd, P. W. & Hutchins, D. A. Understanding the responses of ocean biota to a complex matrix of cumulative anthropogenic change. *Mar. Ecol. Prog. Ser.* **470,** 125–135 (2012).
9. Riebesell, U. & Tortell, P. in *Ocean Acidification* (eds Gattuso, J. P. & Hansen, L.) 99–116 (Oxford Univ. Press, 2011).
10. Hoppe, C. J. M. *et al.* Iron limitation modulates ocean acidification effects on southern ocean phytoplankton communities. *PLoS ONE* **8,** e79890 (2013).

11. Garcia, N. S., Fu, F. X. & Hutchins, D. A. Co-limitation of the unicellular photosynthetic diazotroph *Crocosphaera watsonii* by phosphorus, light and carbon dioxide. *Limnol. Oceanogr.* **58,** 1501–1512 (2013).
12. Boyd, P. W. Beyond ocean acidification. *Nature Geosci.* **4,** 273–274 (2011).
13. Dunne, J. P. A roadmap on ecosystem change. *Nature Clim. Change* **5,** 20–21 (2015).
14. Boyd, P. W., Lennartz, S. T., Glover, D. M. & Doney, S. C. Biological ramifications of climate-change mediated oceanic multi-stressors. *Nature Clim. Change* **5,** 71–79 (2015).
15. Marchetti, A. *et al.* Phytoplankton processes during a mesoscale iron enrichment in the NE subarctic Pacific: Part 1-Biomass and assemblage. *Deep-Sea Res. II* **53,** 2095–2113 (2006).
16. Lehmann, J. T. Interacting growth and loss rates: The balance of top-down and bottom-up controls in plankton communities. *Limnol. Oceanogr.* **36,** 1546–1554 (1991).
17. Smith, W. O. Jr (ed.) *Polar Oceanography, Chemistry, Biology and Geology* 477–517 (Academic Press, 1990).
18. Moore, J. K. *et al.* Marine ecosystem dynamics and biogeochemical cycling in the Community Earth System Model CESM1(BGC). *J. Clim.* **26,** 9291–9321 (2013).
19. Nunn, B. L. *et al.* Diatom proteomics reveals unique acclimation strategies to mitigate Fe limitation. *PLoS ONE* **8,** e75653 (2013).
20. Poulson-Ellestad, K. L. *et al.* Metabolomics and proteomics reveal impacts of chemically mediated competition on plankton. *Proc. Natl Acad. Sci. USA* **111,** 9009–9014 (2014).
21. Fletcher, D. & Dillingham, P. Model-averaged confidence intervals for factorial experiments. *Comput. Stat. Data Anal.* **55,** 3041–3048 (2011).
22. Berges, J. A., Varela, D. E. & Harrison, P. J. Effects of temperature on growth rate, composition and nitrogen metabolism in the marine diatom *Thalassiosira pseudonana* (Bacillariophyceae). *Mar. Ecol. Prog. Ser.* **225,** 139–146 (2002).
23. Strzepek, R. F. & Price, N. M. Influence of irradiance and temperature on the iron content of the marine diatom *Thalassiosira weissflogii*. *Mar. Ecol. Prog. Ser.* **206,** 107–117 (2000).
24. Toseland, A. *et al.* The impact of temperature on marine phytoplankton resource allocation and metabolism. *Nature Clim. Change* **3,** 979–984 (2013).
25. Sugie K. & Yoshimura T. Effects of p_{CO_2} and iron on the elemental composition and geometry of the marine diatom *Pseudo-nitzschia pseudodelicatissima*. *J. Phycol.* **49,** 475–488 (2013).
26. Marchetti, A. & Harrison, P. J. Coupled changes in the cell morphology and the elemental (C, N and Si) composition of oceanic and coastal species of the pennate diatom Pseudo-nitzschia due to iron deficiency. *Limnol. Oceanogr.* **52,** 2270–2284 (2007).
27. Nunn, B. L. *et al.* Deciphering diatom biochemical pathways via whole-cell proteomics. *Aquat. Microb. Ecol.* **55,** 241–253 (2009).
28. Bissinger, J. E., Montagnes, D. J. S., Sharples, J. & Atkinson, D. Predicting marine phytoplankton maximum growth rates from temperature: Improving on the Eppley curve using quantile regression. *Limnol. Oceanogr.* **53,** 487–497 (2008).
29. Boyd, P., LaRoche, J., Gall, M., Frew, R. & McKay, R. M. L. Role of iron, light, and silicate in controlling algal biomass in subantarctic waters SE of New Zealand. *J. Geophys. Res.* **104,** 13395–13408 (1999).
30. Goldman, J. C. & Carpenter, E. J. A kinetic approach to the effect of temperature on algal growth. *Limnol. Oceanogr.* **19,** 756–766 (1974).
31. Price, N. M. The elemental stoichiometry and composition of an iron-limited diatom. *Limnol. Oceanogr.* **50,** 1159–1171 (2005).
32. Martin-Jezequel, V. M., Hildebrand, V. M. & Brzezinki, M. A. Silicon metabolism in diatoms: Implications for growth. *J. Phycol.* **36,** 821–840 (2000).
33. Rose, J. M. *et al.* Synergistic effects of iron and temperature on Antarctic phytoplankton and microzooplankton assemblages. *Biogeosciences* **6,** 3131–3147 (2009).
34. Raven, J. A. & Geider, R. J. Temperature and algal growth. *New Phytol.* **110,** 441–461 (1988).
35. Kolber, Z. S. *et al.* Iron limitation of phytoplankton photosynthesis in the equatorial Pacific Ocean. *Nature* **371,** 145–149 (1994).
36. Morel, F. M. M. & Price, N. M. The biogeochemical cycles of trace metals in the oceans. *Science* **300,** 944–946 (2003).
37. Bertrand, E. M., Saito, M. A., Lee, P. A., Dunbar, R. B. & DiTullio, G. R. Iron limitation of springtime bacterial and phytoplankton community in the Ross Sea: Implications for vitamin B12 nutrition. *Front. Microbiol.* http://dx.doi.org/10.3389/fmicb.2011.00160 (2011).
38. Shi, D. A., Xu, Y., Hopkinson, B. M. & Morel, F. M. M. Effect of ocean acidification on iron availability to marine phytoplankton. *Science* **327,** 676–679 (2010).
39. Sunda, W. G. & Huntsman, S. A. Interactive effects of light and temperature on iron limitation in a marine diatom: Implications for marine productivity and carbon cycling. *Limnol. Oceanogr.* **56,** 1475–1488 (2011).
40. Geider, R. J., MacIntyre, H. L. & Kana, T. M. A dynamic regulatory model of phytoplankton acclimation to light, nutrients, and temperature. *Limnol. Oceanogr.* **43,** 679–694 (1998).
41. Klausmeier, C. A., Litchman, E., Daufresne, T. & Levin, S. A. Phytoplankton stoichiometry. *Ecol. Res.* **23,** 479–485 (2008).
42. Trimborn, S., Brenneis, T., Sweet, E. & Rost, B. Sensitivity of Antarctic phytoplankton species to ocean acidification: Growth, carbon acquisition, and species interaction. *Limnol. Oceanogr.* **58,** 997–1007 (2013).
43. Tew, K. S. *et al.* Effects of elevated CO_2 and temperature on the growth, elemental composition, and cell size of two marine diatoms: Potential implications of global climate change. *Hydrobiologia* **741,** 79–87 (2014).
44. Reinfelder, J. R. Carbon dioxide regulation of nitrogen and phosphorus in four species of marine phytoplankton. *Mar. Ecol. Prog. Ser.* **466,** 57–67 (2012).
45. Burkhardt, S., Zondervan, I. & Riebesell, U. Effect of CO_2 concentration on C:N:P ratio in marine phytoplankton: A species comparison. *Limnol. Oceanogr.* **44,** 683–690 (1999).
46. Boyd, P. W. *et al.* Climate-mediated changes to mixed-layer properties in the Southern Ocean: Assessing the phytoplankton response. *Biogeosciences* **5,** 847–864 (2008).
47. Thomas, M. K., Kremer, C. T., Klausmeier, C. A. & Litchman, E. A global pattern of thermal adaptation in marine phytoplankton. *Science* **741,** 79–87 (2012).
48. Trimborn, S. *et al.* Inorganic carbon acquisition in potentially toxic and non-toxic diatoms: The effect of pH-induced changes in seawater carbonate chemistry. *Physiol. Plant.* **133,** 92–105 (2008).
49. Ou, L. *et al.* Comparative study of phosphorus strategies of three typical harmful algae in Chinese coastal waters. *J. Plank. Res.* **30,** 1007–1017 (2008).
50. Chan, L. L. *et al.* Proteomic study of a model causative agent of harmful algal blooms, Prorocentrum triestinum II: The use of differentially expressed protein profiles under different growth phases and growth conditions for bloom prediction. *Proteomics* **4,** 3214–3226 (2004).

Acknowledgements

P.W.B. acknowledges support from IMAS and the ACE-CRC. C.L.H. received Marsden funding (UOO0914, Royal Society of New Zealand) to support M.Y.R., C.E.C. and Y.-y.F. B.L.N. and E.T.-S. were supported by National Science Foundation grants OCE-1060300 (B.L.N.) and OCE-1233014 (E.T.-S.) and the University of Washington Proteomics Bioinformatics Team (UWPR95794). We thank K.J.M. Dickinson and E. Breitbarth for provision of laboratory culture facilities and expertise in incubation set-up, respectively.

Author contributions

P.W.B. conceived and designed the experiments; E.A.A., C.E.C., C.M.Mc.G., M.Y.R. and P.W.B. performed the experiments; B.L.N. and E.T.-S. conducted the proteomics analysis; P.W.D. developed the statistical experimental design and carried out the biostatistical analysis; C.L.H. and M.R.-G. contributed materials/analysis tools; P.W.B., B.L.N., P.W.D., C.M.Mc.G., E.A.A., C.L.H. and E.T.-S. wrote the paper.

Additional information

Supplementary information is available in the online version of the paper. Reprints and permissions information is available online at www.nature.com/reprints. Correspondence and requests for materials should be addressed to P.W.B.

Competing financial interests

The authors declare no competing financial interests.

Methods

Study organism. *Pseudonitzschia multiseries* ($12 \times 4 \times 3.6\,\mu m$, from scanning electron microscopy; $86.4\,\mu m^3$ (using the 'prism on parallelogram base' geometric shape for biovolume[51])) was isolated in September 2011 from high-nitrate low-chlorophyll subantarctic waters off New Zealand that have low dissolved iron concentrations year-round (that is, $\sim 0.15\,nmol\,l^{-1}$; ref. 29). Pennate diatoms are common in subpolar waters[28–30]. The isolate has since been maintained in unialgal culture in the artificial seawater medium Aquil[52] with a pFe of 19.1, nitrate 300 µM, phosphate 20 µM and silicate 100 µM. Six months before the experiment the diatom was acclimated to pFe 20.0 with the same nutrient concentrations.

Selection of the dominant physiological control on subantarctic diatoms. A review of environmental controls on phytoplankton[6] advocated the use of a physiological ranking scheme to initially identify the dominant control (*sensu*; ref. 16) on phytoplankton groups. They[6] proposed that temperature was likely to be dominant control for Southern Ocean diatoms. To investigate this assertion further we conducted a reaction norm and measured the steady-state growth rate of our subantarctic diatom across 8 temperatures (8–17 °C) using a temperature-controlled aluminium block modified after ref. 53.

Experimental design. Five key properties (temperature/CO_2/nutrients/iron/light) were identified as likely to influence diatom physiology[6]. We employed an efficient experimental design that relies on prior identification of a dominant factor (that is, temperature), and then collapses the non-dominant factors together. This approach balances the needs of making accurate predictions of physiological responses under future oceanic conditions with identifying which factors and interaction terms are most important in driving those responses. This collapsed design allows measurement of the relative importance of: the putative dominant factor; the combination of the other four factors; and the interaction of the dominant factor with the four combined factors.

For our needs, this is an improvement on classical multi-factor designs such as full factorial or fractional factorial designs. Full factorial designs perform well when the number of factors is limited and the aim of a study is to determine which factors and interaction terms are most important. However, they are inefficient for making accurate future predictions and can become intractable with multiple factors. For example, a full 2^5 factorial with three replicates per treatment would have required $32 \times 3 = 96$ experimental units, beyond the current capabilities of even our state-of-the-art manipulation system[54]. Fractional factorial designs (for example, 2^{5-1} designs or smaller)[55] reduce the number of treatments, but are still inefficient for making future predictions because interaction effects are not additive and most treatment combinations do not represent possible future scenarios. Even when some interactions are not important and advanced statistical techniques such as model averaging are employed, many treatments would provide limited or no information for predictions.

After identifying temperature as the dominant factor, it was kept separate and the other four factors were grouped together into a combined factor. We then employed a 2^2 factorial design that provides efficient predictions of future responses (2 of 4 treatments represent plausible current and future factor combinations, rather than 2 of 32 as would occur in a conventional 2^5 design) and maintains experimental balance. Thus, for temperature, we had two levels (current: 10.6 °C; and year 2100 warming: 13.7 °C). For the second factor, we also had two levels (current: CO_2, nutrients, iron, light; year 2100 conditions: CO_2, nutrients, iron, light). This design allows us to resolve between temperature-only effects and the combined interactive effects between temperature and the other four altered properties. For the other altered properties, although we cannot determine the effects of individual properties, we can determine their combined effects (both primary and interactive). Ultimately, this design allowed us to gain insights into the property likely to have the largest influence on physiological response (temperature), and its overall interactions with other properties, and to make holistic predictions for the physiological response of a subantarctic diatom under year 2100 oceanic conditions. This would not be possible from an experiment that did not manipulate all five properties.

Experimental treatments. Two seawater media were used to provide the conditions used for each of four treatments (Table 1). Media preparation, and the prior acclimation of the replicate cultures to the range of growth conditions in Table 1 for treatments A–D followed published procedures. The preparation of media, and the prior acclimation of the replicate cultures to the range of growth conditions presented below for each of the four experimental treatments followed procedures detailed in refs 56,57. The magnitude of the nutrient additions were confirmed by analysis using a QuickChem Automated Ion Analyser (Lachat Instruments). The analysis of CO_2 for the treatments is detailed in Supplementary Methods. Changes in free iron concentration [Fe′] during the experiment were driven by biologically mediated alteration of pH (Supplementary Methods). Treatments A–D were based on model projections for the subantarctic province from the NCAR Community Earth System Model biogeochemical climate-change model[18,46]. The subantarctic is characterized by considerable sub-regional variability in mixed-layer depth (for present-day and future projections)[46]; hence, the irradiances selected were based on those South of New Zealand (Fig. 3 in ref. 46).

Incubation system. The experiment was housed in a walk-in Contherm BIOSYN Series Model 650 Plant Growth Chamber that provided lighting for the experiment and maintained temperature control during subsampling when bottles were removed from temperature-controlled water baths. Following acclimation, the diatom was cultured in $16 \times 2\,l^2$ (trace-metal cleaned, after procedures in ref. 56) polycarbonate culture vessels, comprising four bottles for each treatment; three replicates containing phytoplankton culture and one control abiotic bottle. Target pH levels were achieved by flowing pre-mixed gases through a 10-cm loop of silicone tubing placed through the Teflon lid of each culture vessel[58]. As CO_2 gas flowed through the tubing, it diffused into the sea water, increasing the dissolved inorganic carbon (DIC) and decreasing the pH. This approach achieves target pH levels, while maintaining trace-metal clean conditions within the culture vessels[58,59]. For the ambient p_{CO_2} treatments (A and B), 378 ppm (±8 ppm) CO_2 gas flowed through the tubing of each culture vessel for 40 h. For the high-CO_2 treatments (C and D), 10% CO_2 flowed through the tubing for 10 min, and then 747 ppm (± 15 ppm) CO_2 for 40 h.

Culture vessels were placed in water baths at 10.7 °C and 13.6 °C for accurate control and monitoring of the low-temperature and high-temperature treatments. Low-temperature treatments were cultured for 17 days, and high-temperature treatments for 14 days. Irradiance was continuously monitored using floating PAR (Photosynthetically Active Radiance) sensors within each water bath. Irradiances required for each treatment were modified using neutral density screening to attenuate the plant growth chamber (using a subset of the 24×400 W) metal halide lamps (maximum output of 650 µmol quanta $m^{-2}\,s^{-1}$ using all 24 lamps). A class-100 laminar flow hood was employed within the walk-in growth chamber to provide trace-metal clean conditions.

The lids of the polycarbonate culture vessels were fitted with 5 ports. The first port tubing was fitted with a 0.2 µm syringe filter and was used for bubbling air into the media before inoculation as described above. The second port was also fitted with a 0.2 µm syringe filter and was used to put air into the head space of the culture bottle during the incubation. The third port was fitted with a 0.2 µm filter and left open to allow excess air out of the bottle thereby releasing pressure. The fourth port tubing was for pH sampling and the fifth port was used to sample the other parameters.

Sampling protocols. Bottles were removed from the incubators, and the sampling ports carefully disconnected within the laminar flow hood. The cells were then re-suspended by gently inverting each bottle. Samples for pH were taken after the bottles were returned to the incubator. Sampling for all experimental parameters in each bottle was carried out on day 0, 4 and 9 (all treatments), and then days 11 and 14 for treatments B and D and on day 15 for A and day 17 for A and C. The following protocols were employed at each sampling point.

For cell counts 1 ml samples were fixed with 50% glutaraldehyde to a final concentration of 0.5% and stored at 4 °C. Cells were counted with an Olympus CKX 41 inverted microscope using a 0.1 ml nannoplankton chamber (PhycoTech).

Protocols for *in vivo* and *in vitro* chlorophyll analysis, active fluorescence, and the calculation of chlorophyll-based cell growth rates followed those in refs 56,57.

Cellular particulate C and N were analysed in a Thermo Flash 2000 CHN Elemental Analyser. Particulate P and biogenic Si were analysed following procedures in ref. 60 and ref. 61, respectively, and converted to cellular elemental composition based on cell counts. The low cell abundances in treatment C resulted in some assays being close to the limits of detection and in some cases being lower than the blanks. No subsamples were taken for dissolved iron analysis during the experiment, but confirmation of no trace-metal contamination of the treatments was obtained indirectly by monitoring several physiological metrics—such as C/chlorophyll, growth rate or cellular silica (see Supplementary Table 4)—that are sensitive to iron supply.

Measurement of pH and DIC. In our study, we permitted the initial p_{CO_2} to be biologically altered during the course of the experiment by the diatom physiology. In our study, B and D were the only treatments with a measurable change in DIC over the course of the experiment. In treatment B, the DIC decreased by 183 (39) µmol kg^{-1}; in treatment D, DIC decreased by 519 (31) µmol kg^{-1}.

Automated pH_T measurements were made daily using the spectrophotometric pH measurement system described in ref. 54. Briefly, syringe pumps and rotary valves (Norgren Kloehn) were used to sample sea water from individual culture vessels and mix it with thymol blue indicator dye. This solution was directed to an Ocean Optics spectrometer (USB4000) where absorbance measurements were used to determine pH using the method of ref. 62. The automated control of all instruments and the calculation of pH_T were done using LabVIEW (National Instruments).

pH_T was measured each day, and samples for DIC were obtained at the same time as those for other parameters. Samples were preserved with saturated mercuric chloride and analysed using an AIRICA IR-based detection system (Marianda). In treatment B, the DIC decreased by 183 (ref. 39) μmol kg^{-1}; in treatment D, DIC decreased by 519 μmol kg^{-1}. Carbonate chemistry calculations were done in $SWCO_2$ (ref. 63) using the dissociation constants[64], refitted by ref. 65. The change in carbonate chemistry within the abiotic controls for treatments A–D was relatively small over the course of the experiment compared with the diatom cultures.

Proteomic profiling and quantitative analysis. Data-dependent tandem mass spectrometry was carried out on a Thermo Scientific Q-Exactive tandem mass spectrometer following protocols detailed in ref. 20. Relative abundances of proteins across all biological replicates of treatments A–D were determined using spectral counting[19,66]. Normalized spectral abundance factors (NSAF) were calculated using ABACUS software on all data sets[67]. NSAF values were then statistically evaluated using QSPEC (ref. 66). Protein abundance values (adjusted normalized spectral abundance factor, Data set S1) were $\log(x+1)$ transformed for the NMDS analysis and a Bray–Curtis dissimilarity matrix was used to construct the NMDS. The NMDS presented in Fig. 5a employed a statistically significant separation among samples based on treatment calculated using ANOSIM in the vegan package (688) in R (ref. 68) version 3.1.0 ($R=0.9689$).

In addition, the peak intensity integrations for tryptic peptides, resulting from 26 proteins determined to be significantly different using spectral counting were further analysed using MS1 full-scan filtering to validate relative abundances[69]. These proteins were chosen to be examined for comparative quantification using peptide chromatographic peak intensity. Proteins chosen to have a secondary quantitative analysis using MS1 full-scan filtering were either significantly more or less abundant on the basis of spectral counting comparisons of treatments A versus C, A versus D, and C versus D using QSpec statistical analysis[66]. These proteins were used as the background proteome in Skyline daily v. 2.6.1.7171 (refs 69,70) for protein and peptide quantification by MS1 full-scan filtering. A standard method for unbiased protein quantification from a whole cell employs spectral counting, which allows relative quantification of all proteins identified. That said, spectral counting relies on the detection of MS2 spectra and thus risks underreporting lower-abundance peptides. MS1 full-scan filtering relies on measuring the relative peak intensities of MS1 peptide intensities and is both accurate and precise over time[69]. Duplicate peptides were removed from the analysis as well as peptides with poor-quality spectra across most biological and technical replicates. Differentially abundant proteins were detected using the R v. 3.1.1 package MSstats (refs 71,72). In MSstats, scope of biological replicates was set to expanded (the more conservative approach) and scope of technical replicates was set to restricted. The consistency between spectral counting and the MS1 full-scan filtering method provided further unbiased confirmation on the physiological importance of the 26 proteins examined.

Statistical analysis. We employed a 2^2 factorial design where one factor was temperature (set at current and year 2100 levels) and the other factor collapsed four stressors at current and future levels. When estimating treatment means, differences in treatment means, standard errors and confidence intervals, model averaging was employed to optimize the bias-variance trade-off[21].

Determining the importance of various factors in an experiment or research study has traditionally been done through hypothesis-based analysis methods such as analysis of variance, but can also be performed in a model selection context[73]. There is a preference towards this latter approach representing a broad trend in ecological research[74]. In model selection, a suite of statistical models are fitted to the data (that is, various factors are included or not included in different models) and their relative performance is compared using some metric, such as Akaike's information criterion[73] (AIC). In addition to the philosophical advantage of separating model fit from hypothesis testing[74], predictions that do not ignore the uncertainty and variance inherent to the model selection process (for example, model-averaged predictions based on AIC) outperform those that do[21,75–77]. In this study, we used five linear regression-based statistical models (M1 to M5) to determine the relative importance of temperature, the combined other factors, and their interaction (see main text).

For each physiological metric and each model, AIC was calculated. AIC measures how well each statistical model fits the data, but also has a penalty for the number of factors included. Two (or more) models can be compared by examining the differences in AIC between them (ΔAIC); if $\Delta\text{AIC} > 2$, the model with lower AIC is considered to be superior, whereas differences between 0 and 2 are considered equivocal. Across all of the statistical models, AIC can also be converted into AIC weights (AIC_w), which measure the level of support for each model, where 0 = no support, 1 = full support, and the sum of AIC weights across all models is 1; ΔAIC and AIC_w are shown in Supplementary Table 3. For example, for the primary metrics of growth rate and cell count, M5 (the full model that includes all factors and their interactions) fits the data much better than models M2 and M4 ($\Delta\text{AIC} > 10$ for each), which strongly outperformed models M1 and M3 ($\Delta\text{AIC} > 6$ for each). Nearly all ($AIC_w > 0.99$) support was on M5 for each metric, with most support on the most complex model for the secondary metrics as well (Supplementary Table 3). AIC weights were also used to estimate model-averaged treatment means and differences between treatments, their standard errors and approximate 95% confidence intervals[21], shown in Supplementary Table 1. Finally, the resulting model-averaged confidence intervals were used in statements that two groups were distinguishable from each other (for example, a statement such as A>B implies that the lower limit of the 95% model-averaged confidence interval for A–B was >0).

Although we were able to quantify growth rate and cell counts for all experimental units (replicates), the weak physiological performance (that is, low cell counts) exhibited by treatment C limited our ability to quantify the secondary metrics of cellular C, N, P and Si. We therefore removed two replicates each with low cell counts for the estimation of cellular C, N, P and Si. For cellular chlorophyll, the variation in treatment C was much greater than in the other treatments, violating the model assumption of homogeneous treatment variances required for model-averaged confidence intervals. Therefore, confidence intervals for treatment C and its comparisons with other treatments were calculated using robust t-based confidence intervals[78] where treatments A, B and D were considered to have a common variance different from that of treatment C.

As a descriptive statistic, we also calculated partial-R^2 to describe variation explained by model components. For example, for M5, partial-R^2 describes the proportion of variation explained (0 = none; 1 = all explained) by temperature alone, the other four altered properties alone, and the interaction of the two (Fig. 4). For example, for growth rate, temperature explained 80% of the observed variation by itself. However, the interaction between temperature and the other altered properties explained 2/3 of the remaining variation (13% of 20%). For those metrics with high AIC weight on M5 and a large partial-R^2 for the interaction term, it is important to incorporate all important factors at ambient and predicted future levels, and allowing for the complex interplay between them, to correctly estimate anthropogenic effects.

Principal components analysis. As many of the physiological metrics were highly positively or negatively correlated with each other, a principal components analysis (PCA) was undertaken to examine the underlying structure of the variables at reduced dimensionality. The PCA was conducted using the following variables, each rescaled to have mean 0 and unit standard deviation: chlorophyll-derived growth rate, log n (cell count), chlorophyll a, log C, log N, log P and log Si. Two observations in treatment C had cell counts that were too low for accurate measurement of cellular N, P and Si and were therefore excluded from the PCA.

References

51. Hillebrand, H. *et al.* Biovolume calculation for pelagic and benthic microalgae. *J. Phycol.* **35,** 403–424 (1999).
52. Price, N. M. *et al.* Preparation and chemistry of the artificial algal culture medium Aquil. *Biol. Oceanogr.* **6,** 443–461 (1988/89).
53. Thomas, W. H., Scotten, H. L. & Bradshaw, J. S. Thermal gradient incubators for small aquatic organisms. *Limnol. Oceanogr.* **8,** 357–360 (1963).
54. McGraw, C. M. *et al.* An automated pH-controlled culture system for laboratory-based ocean acidification experiments. *Limnol. Oceanogr.* **8,** 686–694 (2010).
55. Box, G. E. P., Hunter, W. G. & Hunter, J. S. *Statistics for Experimenters: An Introduction to Design, Data Analysis, and Model Building* (Wiley, 1978).
56. Strzepek, R. F., Maldonado, M. T., Hunter, K. A., Frew, R. D. & Boyd, P. W. Adaptive strategies by Southern Ocean phytoplankton to lessen iron limitation: Uptake of organically complexed iron and reduced cellular iron requirements. *Limnol. Oceanogr.* **56,** 1983–2002 (2011).
57. Strzepek, R. F., Hunter, K. A., Frew, R. D., Harrison, P. J. & Boyd, P. W. Iron-light interactions differ in Southern Ocean phytoplankton. *Limnol. Oceanogr.* **57,** 1182–1200 (2012).
58. Hoffmann, L. J. *et al.* A trace-metal clean, pH-controlled incubator system for ocean acidification incubation studies. *Limnol. Oceanogr.* **11,** 53–61 (2013).
59. Law, C. S. *et al.* No stimulation of nitrogen fixation by non-filamentous diazotrophs under elevated CO_2 in the South Pacific. *Glob. Change Biol.* **18,** 3004–3014 (2012).
60. Paasche, E. Silicon and the ecology of marine plankton diatoms. I. *Thalassiosira pseudonana* (*Cyclotella nana*) grown in chemostat with silicate as limiting nutrient. *Mar. Biol.* **19,** 117–126 (1973).
61. Solórzano, L. & Sharp, J. H. Determination of total dissolved phosphorus and particulate phosphorus in natural waters. *Limnol. Oceanogr.* **25,** 754–758 (1980).
62. Zhang, H. N. & Byrne, R. H. Spectrophotometric pH measurements of surface seawater at *in-situ* conditions: Absorbance and protonation behavior of thymol blue. *Mar. Chem.* **52,** 17–25 (1996).

63. Hunter, K. A. SWCO2; http://neon.otago.ac.nz/research/mfc/people/keith_hunter/software/swco2 (2009).
64. Mehrbach, C., Culberson, C. H., Hawley, J. E. & Pytkowicz, R. M. Measurement of the apparent dissociation constants of carbonic acid in seawater at atmospheric pressure. *Limnol. Oceanogr.* **18,** 897–907 (1973).
65. Dickson, A. G. & Millero, F. J. A comparison of the equilibrium-constants for the dissociation of carbonic-acid in seawater media. *Deep-Sea Res. I* **34,** 1733–1743 (1987).
66. Choi, H., Fermin, D. & Nesvizhskii, A. Significance analysis of spectral count data in label-free shotgun proteomics. *Mol. Cell Proteomics* **7,** 2373–2385 (2008).
67. Fermin, D., Basrur, V., Yocum, A. K. & Nesvizhskii, A. I. Abacus: A computational tool for extracting and pre-processing spectral count data for label-free quantitative proteomic analysis. *Proteomics* **11,** 1340–1345 (2011).
68. Oksanen, J. *et al. vegan: Community Ecology Package* R package version 2.0-8 (2013); http://www.bioconductor.org/packages/release/bioc/html/MSstats.html
69. Schilling, B. *et al.* Platform-independent and label-free quantitation of proteomic data using MS1 extracted ion chromatograms in skyline: Application to protein acetylation and phosphorylation. *Mol. Cell Proteomics* **11,** 202–214 (2012).
70. R Core Team *R: A Language and Environment for Statistical Computing* (Foundation for Statistical Computing, 2014); http://www.R-project.org
71. MacLean, B. D. M. *et al.* Skyline: An open source document editor for creating and analyzing targeted proteomics experiments. *Bioinformatics* **26,** 966–968 (2010).
72. Choi, M., Chang, C.-Y. & Vitek, O. *MSstats.daily: Protein Significance Analysis in DDA, SRM and DIA for Label-free or Label-based Proteomics Experiments* R package version 2.3.5 (2014).
73. Burnham, K. P. & Anderson, D. R. *Model Selection and Multimodel Inference: A Practical Information-Theoretic Approach* 2nd edn (Springer, 2002).
74. Link, W. A. & Barker, R. J. Model weights and the foundations of multimodel inference. *Ecology* **87,** 2626–2635 (2006).
75. Chatfield, C. Model uncertainty, data mining and statistical inference. *J. R. Stat. Soc. Ser. A* **158,** 419–466 (1995).
76. Buckland, S. T., Burnham, K. P. & Augustin, N. H. Model selection: An integral part of inference. *Biometrics* **53,** 603–618 (1997).
77. Turek, D. & Fletcher, D. Model-averaged Wald confidence intervals. *Comput. Stat. Data Anal.* **56,** 2809–2815 (2012).
78. Welch, B. L. The generalization of Student's problem when several different population variances are involved. *Biometrika* **34,** 28–35 (1947).
79. Sieracki, M. E., Verity, P. G. & Stoecker, D. K. Plankton community response to sequential silicate and nitrate depletion during the 1989 North Atlantic spring bloom. *Deep-Sea Res. II* **40,** 213–225 (1993).
80. Allen, J. T. *et al.* Diatom carbon export enhanced by silicate upwelling in the northeast Atlantic. *Nature* **437,** 728–732 (2005).